
Ridge Regression and Provable Deterministic Ridge Leverage Score Sampling

SHANNON R. MCCURDY*

smccurdy@berkeley.edu

Abstract

Ridge leverage scores provide a balance between low-rank approximation and regularization, and are ubiquitous in randomized linear algebra and machine learning. Deterministic algorithms are also of interest in the moderately big data regime, because deterministic algorithms provide interpretability to the practitioner by having no failure probability and always returning the same results.

We provide provable guarantees for deterministic column sampling using ridge leverage scores. The matrix sketch returned by our algorithm is a column subset of the original matrix, yielding additional interpretability. Like the randomized counterparts, the deterministic algorithm provides $(1 + \epsilon)$ error column subset selection, $(1 + \epsilon)$ error projection-cost preservation, and an additive-multiplicative spectral bound. We also show that under the assumption of power-law decay of ridge leverage scores, this deterministic algorithm is provably as accurate as randomized algorithms.

Lastly, ridge regression is frequently used to regularize ill-posed linear least-squares problems. While ridge regression provides shrinkage for the regression coefficients, many of the coefficients remain small but non-zero. Performing ridge regression with the matrix sketch returned by our algorithm and a particular regularization parameter forces coefficients to zero and has a provable $(1 + \epsilon)$ bound on the statistical risk. As such, it is an interesting alternative to elastic net regularization. Column subset selection; Deterministic sampling algorithms; Projection-cost preservation; Ridge leverage scores; Spectral bounds

1 Introduction

Classical leverage scores quantify the importance of each column i for the range space of the sample-by-feature data matrix $\mathbf{A} \in \mathbb{R}^{n \times d}$. Classical leverage scores have been used in regression diagnostics, outlier detection, and randomized matrix algorithms (Velleman and Welsch, 1981; Chatterjee and Hadi, 1986; Drineas et al., 2008).

There are many different flavors of leverage scores, and we will focus on ridge leverage scores. To understand the advantages of ridge leverage scores, we briefly review classical and rank- k subspace leverage scores. A comprehensive review of the extensive leverage score literature is beyond the scope of this note.

Ridge leverage scores were introduced by Alaoui and Mahoney (2015) to give statistical bounds for the Nyström approximation for kernel ridge regression. The ridge leverage score $\bar{\tau}_i(\mathbf{A})$ for the i^{th} column of \mathbf{A} is,

$$\bar{\tau}_i(\mathbf{A}) = \mathbf{a}_i^T (\mathbf{A}\mathbf{A}^T + \lambda_2 \mathbf{I})^+ \mathbf{a}_i, \quad (1)$$

where the i^{th} column of \mathbf{A} is an $(n \times 1)$ -vector denoted by \mathbf{a}_i , \mathbf{M}^+ denotes the Moore-Penrose pseudoinverse of \mathbf{M} , and \mathbf{A}_k is the rank- k SVD approximation to \mathbf{A} , defined in Sec. 5.1, and λ_2 is

the regularization parameter. We will always choose $\lambda_2 = \frac{1}{k} \|\mathbf{A} - \mathbf{A}_k\|_F^2$, because this choice of regularization parameter gives the stated guarantees. In contrast to ridge leverage scores, the rank- k subspace leverage score $\tau_i(\mathbf{A}_k)$ is,

$$\tau_i(\mathbf{A}_k) = \mathbf{a}_i^T (\mathbf{A}_k \mathbf{A}_k^T)^+ \mathbf{a}_i. \quad (2)$$

The classical leverage score is the ridge leverage score (and also the rank- k subspace leverage score) evaluated at $k = \text{rank}(\mathbf{A}) = r \leq n$.

Ridge leverage scores and rank- k subspace leverage scores take two different approaches to mitigating the small principle components of \mathbf{A} in classical leverage scores. Ridge leverage scores diminish the importance of small principle components through regularization, as opposed to rank- k subspace leverage scores, which omit the small principle components entirely. [Cohen et al. \(2017\)](#) argue that regularization is a more natural and stable alternative to omission, and they prove sampling bounds for column subset selection, projection-cost preservation, and the spectrum for randomized algorithms with ridge leverage score sampling. The latter two bounds hold for a weighted column subset of the full data matrix. These bounds require $O(k \log(k/\delta)/\epsilon^2)$ columns, where δ is the failure probability and ϵ is the error.

In the "big data" era, much attention has been paid to randomized algorithms due to improved algorithm performance and ease of generalization to the streaming setting. However, for moderately big data (i.e. the feature set is too large for inspection by humans, but the algorithm performance is not a limitation), deterministic algorithms provide more interpretability to the practitioner than randomized algorithms, since they always provide the same results and have no failure probability.

The usefulness of deterministic algorithms has already been recognized. [Papailiopoulos et al. \(2014\)](#) introduce a deterministic algorithm for sampling columns from rank- k subspace leverage scores and provide a columns subset selection bound. [McCurdy et al. \(2017\)](#) prove a $(1 + \epsilon)$ spectral bound for [Papailiopoulos et al. \(2014\)](#)'s deterministic algorithm and for random sampling with rank- k subspace leverage scores. However, the relative spectral bound is limited to the rank- k subspace projection of the column subset matrix \mathbf{C} and the full data matrix \mathbf{A} , so to get a comparable relative spectral bound requires $k = n$. On the other hand, under the condition of power-law decay in the sorted rank- k subspace leverage scores, the deterministic algorithm chooses fewer columns than random sampling with the same error for the column subset selection bound when $\max((2k/\epsilon)^{\frac{1}{a}} - 1, (2k/((a-1)\epsilon))^{\frac{1}{a-1}} - 1, k) < Ck \log(k/\delta)/\epsilon^2$, where a is the decay power and C is an absolute constant ([Papailiopoulos et al., 2014](#)). In addition, [Papailiopoulos et al. \(2014\)](#) show that many real data sets display power-law decay in the sorted rank- k subspace leverage scores, illustrating the algorithm's real-world utility.

Ridge regression ([Hoerl and Kennard, 1970](#)) is a commonly used method to regularize ill-posed linear least-squares problems. The ridge regression minimization problem is, for outcome $\mathbf{y} \in \mathbb{R}^n$, features $\mathbf{A} \in \mathbb{R}^{n \times d}$, and coefficients $\mathbf{x} \in \mathbb{R}^n$,

$$\begin{aligned} \hat{\mathbf{x}}_{\mathbf{A}} &= \underset{\mathbf{x}}{\operatorname{argmin}} (\|\mathbf{y} - \mathbf{A}\mathbf{x}\|_2^2 + \lambda_2 \|\mathbf{x}\|_2^2) \\ &= (\mathbf{A}^T \mathbf{A} + \lambda_2 \mathbf{I})^{-1} \mathbf{A}^T \mathbf{y}. \end{aligned} \quad (3)$$

where the regularization parameter λ_2 penalizes the size of the coefficients in the minimization problem. We will always choose $\lambda_2 = \frac{1}{k} \|\mathbf{A} - \mathbf{A}_k\|_F^2$ for ridge regression with matrix \mathbf{A} .

In ridge regression, the underlying statistical model for data generation is,

$$\mathbf{y} = \mathbf{y}^* + \sigma^2 \boldsymbol{\xi}, \quad (4)$$

where $\mathbf{y}^* = \mathbf{A}\mathbf{x}^*$ is a deterministic linear function of the features and $\boldsymbol{\xi} \sim \mathcal{N}(0, \mathbf{I})$ is the random error. The mean squared error is a measure of statistical risk $\mathcal{R}(\hat{\mathbf{y}})$ for the squared error loss function and estimator $\hat{\mathbf{y}}$ and is,

$$\mathcal{R}(\hat{\mathbf{y}}) = \frac{1}{n} \mathbb{E}_{\boldsymbol{\xi}} [\|\hat{\mathbf{y}} - \mathbf{y}^*\|_2^2]. \quad (5)$$

Ridge regression is often chosen over regression subset selection procedures for regularization because, as a continuous shrinkage method, it exhibits lower variability ([Breiman, 1996](#)). However many ridge regression coefficients can be small but non-zero, leading to a lack of interpretability for moderately big data ($d > n$). The lasso method ([Tibshirani, 1994](#)) provides continuous shrinkage

and automatic feature selection using an L_1 penalty function instead of the L_2 penalty function in ridge regression, but for $d > n$ case, lasso saturates at n features. The elastic net algorithm combines lasso (L_1 penalty function) and ridge regression (L_2 penalty function) for continuous shrinkage and automatic feature selection (Zou and Hastie, 2005). We combine deterministic ridge leverage score column subset selection with ridge regression for a particular value of the regularization parameter, providing automatic feature selection and continuous shrinkage, and we show that the statistical risk is bounded.

1.1 Contributions

We introduce a deterministic algorithm (Algorithm 1) for ridge leverage score column sampling inspired by the deterministic algorithm of Papailiopoulos et al. (2014). By using ridge leverage scores instead of rank- k subspace scores in the deterministic algorithm, we can prove additional nice bounds for the column subset matrix \mathbf{C} . We prove that the same $(1 + \epsilon)$ columns subset selection, $(1 + \epsilon)$ projection-cost preservation, and additive-multiplicative spectral bounds hold for deterministic column sampling as for random sampling as in Cohen et al. (2017). We show that under the condition of power-law decay in the ridge leverage scores, the deterministic algorithm chooses fewer columns than random sampling with the same error when $\max((4k/\epsilon)^{\frac{1}{a}} - 1, (4k/((a-1)\epsilon))^{\frac{1}{a-1}} - 1, k) < Ck \log(k/\delta)/\epsilon^2$, where a is the decay power and C is an absolute constant. We show that ridge regression performed with the column subset matrix \mathbf{C} and a particular choice of regularization parameter has a provable $(1 + \epsilon)$ bound on the statistical risk. The proof techniques are such that a $(1 + \epsilon)$ bound on the statistical risk also holds for randomized ridge leverage score sampling as in Cohen et al. (2017). We also provide a proof-of-concept illustration on biological data.

Our work is triply beneficial from the interpretability standpoint; it is deterministic, it chooses an unweighted subset of representative columns, and it comes with four desirable error guarantees, three of which stem from naturalness of the low-rank ridge regularization.

1.2 Notation

The *singular value decomposition* (SVD) of any complex matrix \mathbf{A} is $\mathbf{A} = \mathbf{U}\Sigma\mathbf{V}^\dagger$, where \mathbf{U} and \mathbf{V} are square unitary matrices ($\mathbf{U}^\dagger\mathbf{U} = \mathbf{U}\mathbf{U}^\dagger = \mathbf{I}$, $\mathbf{V}^\dagger\mathbf{V} = \mathbf{V}\mathbf{V}^\dagger = \mathbf{I}$), Σ is a rectangular diagonal matrix with real non-negative non-increasingly ordered entries. \mathbf{U}^\dagger is the complex conjugate and transpose of \mathbf{U} , and \mathbf{I} is the identity matrix. The diagonal elements of Σ are called the *singular values*, and they are the positive square roots of the eigenvalues of both $\mathbf{A}\mathbf{A}^\dagger$ and $\mathbf{A}^\dagger\mathbf{A}$, which have eigenvectors \mathbf{U} and \mathbf{V} , respectively. \mathbf{U} and \mathbf{V} are the *left* and *right singular vectors* of \mathbf{A} .

Defining \mathbf{U}_k as the first k columns of \mathbf{U} and analogously for \mathbf{V} , and Σ_k the square diagonal matrix with the first k entries of Σ , then $\mathbf{A}_k = \mathbf{U}_k \Sigma_k \mathbf{V}_k^\dagger$ is the rank- k SVD approximation to \mathbf{A} . Furthermore, we refer to matrix with only the last $n - k$ columns of \mathbf{U} , \mathbf{V} and last $n - k$ entries in Σ as $\mathbf{U}_{\setminus k}$, $\mathbf{V}_{\setminus k}$, and $\Sigma_{\setminus k}$.

The Moore-Penrose pseudo inverse of a rank r matrix \mathbf{A} is given by $\mathbf{A}^+ = \mathbf{V}_r \Sigma_r^{-1} \mathbf{U}_r^\dagger$.

The Frobenius norm $\|\mathbf{A}\|_F$ of a matrix \mathbf{A} is given by $\|\mathbf{A}\|_F^2 = \text{tr}(\mathbf{A}\mathbf{A}^\dagger)$. The spectral norm $\|\mathbf{A}\|_2$ of a matrix \mathbf{A} is given by the largest singular value of \mathbf{A} .

2 Deterministic Ridge Column Sampling

2.1 The DRLS Algorithm

Algorithm 1. *The DRLS algorithm selects for the submatrix \mathbf{C} all columns i with ridge leverage score $\bar{\tau}_i(\mathbf{A})$ above a threshold θ , determined by the error tolerance ϵ . The algorithm is as follows.*

1. Choose the error tolerance, ϵ .
2. For every column i , calculate the ridge leverage scores $\bar{\tau}_i(\mathbf{A})$ (Eqn. 1).
3. Sort the columns by $\bar{\tau}_i(\mathbf{A})$, from largest to smallest. The sorted column indices are π_i .

4. Define an empty set $\Theta = \{\}$. Starting with the largest sorted column index π_0 , add the corresponding column index i to the set Θ , in decreasing order, until,

$$\sum_{i \in \Theta} \bar{\tau}_i(\mathbf{A}) > \bar{t} - \epsilon, \quad (6)$$

and then stop. Note that $\bar{t} = \sum_{i=1}^d \bar{\tau}_i(\mathbf{A}) \leq 2k$ (see Sec. 5.2 for proof). It will be useful to define $\tilde{\epsilon} = \sum_{i \notin \Theta} \bar{\tau}_i(\mathbf{A})$. Eqn. 6 can equivalently be written as $\epsilon > \tilde{\epsilon}$.

5. If the set size $|\Theta| < k$, continue adding columns in decreasing order until $|\Theta| = k$.
6. The leverage score $\bar{\tau}_i(\mathbf{A})$ of the last column i included in Θ defines the leverage score threshold θ .
7. Introduce a rectangular selection matrix \mathbf{S} of size $d \times |\Theta|$. If the column indexed by (i, π_i) is in Θ , then $\mathbf{S}_{i, \pi_i} = 1$. $\mathbf{S}_{i, \pi_i} = 0$ otherwise. The DRLS submatrix is $\mathbf{C} = \mathbf{A}\mathbf{S}$.

Note that when the ridge leverage scores on either side of the threshold are not equal, the algorithm returns a unique solution. Otherwise, there are as many solutions as there are columns with equal ridge leverage scores at the threshold.

This algorithm is deeply indebted to the deterministic algorithm of Papailiopoulos et al. (2014). It substitutes ridge leverage scores for rank- k subspace scores, and has a different stopping parameter.

Algorithm 1 requires $O(\min(d, n)nd)$ arithmetic operations.

3 Approximation Guarantees

3.1 Bounds for DRLS

We derive a new additive-multiplicative spectral approximation bound (Eqn. 7) for the square of the submatrix \mathbf{C} selected with DRLS.

Theorem 1. *Additive-Multiplicative Spectral Bound: Let $\mathbf{A} \in \mathbb{R}^{n \times d}$ be a matrix of at least rank k and $\bar{\tau}_i(\mathbf{A})$ be defined as in Eqn. 1. Construct \mathbf{C} following the DRLS algorithm described in Sec. 2.1. Then \mathbf{C} satisfies,*

$$(1 - \epsilon)\mathbf{A}\mathbf{A}^T - \frac{\epsilon}{k}\|\mathbf{A}_{\setminus k}\|_F^2 \mathbf{I} \preceq \mathbf{C}\mathbf{C}^T \preceq \mathbf{A}\mathbf{A}^T. \quad (7)$$

The symbol \preceq denotes the Loewner partial ordering which is reviewed in Sec 5.1 (see Horn and Johnson (2013) for a thorough discussion).

Conceptually, the Loewner ordering in Eqn. 7 is the generalization of the ordering of real numbers (e.g. $1 < 1.5$) to Hermitian matrices. Statements of Loewner ordering are quite powerful; important consequences include inequalities for the eigenvalues. We will use Eqn. 7 to prove Theorems 2, 3, and 4. Note that our additive-multiplicative bound holds for an un-weighted column subset of \mathbf{A} .

Theorem 2. *Column Subset Selection: Let $\mathbf{A} \in \mathbb{R}^{n \times d}$ be a matrix of at least rank k and $\bar{\tau}_i(\mathbf{A})$ be defined as in Eqn. 1. Construct \mathbf{C} following the DRLS algorithm described in Sec. 2.1. Then \mathbf{C} satisfies,*

$$\|\mathbf{A} - \mathbf{C}\mathbf{C}^+ \mathbf{A}\|_F^2 \leq \|\mathbf{A} - \mathbf{\Pi}_{\mathbf{C}, k}^F(\mathbf{A})\|_F^2 \leq (1 + 4\epsilon)\|\mathbf{A}_{\setminus k}\|_F^2, \quad (8)$$

with $0 < \epsilon < \frac{1}{4}$ and where $\mathbf{\Pi}_{\mathbf{C}, k}^F(\mathbf{A}) = (\mathbf{C}\mathbf{C}^+ \mathbf{A})_k$ is the best rank- k approximation to \mathbf{A} in the column space of \mathbf{C} with respect to the Frobenius norm.

Column subset selection algorithms are widely used for feature selection for high-dimensional data, since the aim of the column subset selection problem is to find a small number of columns of \mathbf{A} that approximate the column space nearly as well as the top k singular vectors.

Theorem 3. *Rank- k Projection-Cost Preservation: Let $\mathbf{A} \in \mathbb{R}^{n \times d}$ be a matrix of at least rank k and $\bar{\tau}_i(\mathbf{A})$ be defined as in Eqn. 1. Construct \mathbf{C} following the DRLS algorithm described in Sec. 2.1. Then \mathbf{C} satisfies, for any rank k orthogonal projection $\mathbf{X} \in \mathbb{R}^{n \times n}$,*

$$(1 - \epsilon)\|\mathbf{A} - \mathbf{X}\mathbf{A}\|_F^2 \leq \|\mathbf{C} - \mathbf{X}\mathbf{C}\|_F^2 \leq \|\mathbf{A} - \mathbf{X}\mathbf{A}\|_F^2. \quad (9)$$

To simplify the bookkeeping, we prove the lower bound of Theorem 3 with $(1 - \alpha\epsilon)$ error ($\alpha > 1$), and assume $0 < \epsilon < \frac{1}{2}$.

Projection-cost preservation bounds were formalized recently in [Feldman et al. \(2013\)](#); [Cohen et al. \(2015\)](#). Bounds of this type are important because it means that low-rank projection problems can be solved with \mathbf{C} instead of \mathbf{A} while maintaining the projection cost. Furthermore, the projection-cost preservation bound has implications for k -means clustering, because the k -means objective function can be written in terms of the orthogonal rank- k cluster indicator matrix ([Boutsidis et al., 2009](#)).¹ Note that our rank- k projection-cost preservation bound holds for an un-weighted column subset of \mathbf{A} .

A useful lemma on an approximate ridge leverage score kernel comes from combining Theorem 1 and 3.

Lemma 1. *Approximate ridge leverage score kernel: Let $\mathbf{A} \in \mathbb{R}^{n \times d}$ be a matrix of at least rank k and $\bar{\tau}_i(\mathbf{A})$ be defined as in Eqn. 1. Construct \mathbf{C} following the DRLS algorithm described in Sec. 2.1. Let α be the coefficient in the lower bound of Theorem 3 and assume $0 < \epsilon < \frac{1}{2}$. Let $\mathbf{K}(\mathbf{M}) = (\mathbf{M}\mathbf{M}^T + \frac{1}{k}\|\mathbf{M}_{\setminus k}\|_F^2\mathbf{I})^+$ for matrix $\mathbf{M} \in \mathbb{R}^{n \times l}$. Then $\mathbf{K}(\mathbf{C})$ and $\mathbf{K}(\mathbf{A})$ satisfy,*

$$\mathbf{K}(\mathbf{A}) \preceq \mathbf{K}(\mathbf{C}) \preceq \frac{1}{1 - (\alpha + 1)\epsilon} \mathbf{K}(\mathbf{A}). \quad (10)$$

Theorem 4. *Approximate Ridge Regression with DRLS: Let $\mathbf{A} \in \mathbb{R}^{n \times d}$ be a matrix of at least rank k and $\bar{\tau}_i(\mathbf{A})$ be defined as in Eqn. 1. Construct \mathbf{C} following the DRLS algorithm described in Sec. 2.1, let α be the coefficient in the lower bound of Theorem 3, and assume $0 < \epsilon < \frac{1}{2\alpha} < \frac{1}{2}$. Choose the regularization parameter $\lambda_2 = \frac{\|\mathbf{M}_{\setminus k}\|_F^2}{k}$ for ridge regression with a matrix \mathbf{M} (Eqn. 3). Under these conditions, the statistical risk $\mathcal{R}(\hat{\mathbf{y}}_{\mathbf{C}})$ of the ridge regression estimator $\hat{\mathbf{y}}_{\mathbf{C}}$ is bounded by the statistical risk $\mathcal{R}(\hat{\mathbf{y}}_{\mathbf{A}})$ of the ridge regression estimator $\hat{\mathbf{y}}_{\mathbf{A}}$:*

$$\mathcal{R}(\hat{\mathbf{y}}_{\mathbf{C}}) \leq (1 + \beta\epsilon)\mathcal{R}(\hat{\mathbf{y}}_{\mathbf{A}}), \quad (11)$$

where $\beta = \frac{2\alpha(-1+2\alpha+3\alpha^2)}{(1-\alpha)^2}$.

Theorem 4 means that there are bounds on the statistical risk for substituting the DRLS selected column subset matrix for the complete matrix when performing ridge regression with the appropriate regularization parameter. Performing ridge regression with the column subset \mathbf{C} effectively forces coefficients to be zero and adds the benefits of automatic feature selection to the L_2 regularization problem. We also note that the proof of Theorem 4 relies only on Theorem 2 and Theorem 3 and facts from linear algebra, so a randomized selection of weighted column subsets that obey similar bounds to Theorem 2 and Theorem 3 (e.g. [Cohen et al. \(2017\)](#)) will also have bounded statistical risk, albeit with a different coefficient β . As a point of comparison, consider the elastic net minimization with our ridge regression regularization parameter:

$$\hat{\mathbf{x}}^E = \underset{\mathbf{x}}{\operatorname{argmin}} \left(\|\mathbf{y} - \mathbf{A}\mathbf{x}\|_2^2 + \frac{1}{k}\|\mathbf{A}_{\setminus k}\|_F^2\|\mathbf{x}\|_2^2 + \lambda_1 \sum_{j=1}^d |\mathbf{x}_j| \right). \quad (12)$$

The risk of elastic net $\mathcal{R}(\hat{\mathbf{y}}^E)$ has the following bound in terms of the risk of ridge regression $\mathcal{R}(\hat{\mathbf{y}}_{\mathbf{A}})$:

$$\mathcal{R}(\hat{\mathbf{y}}^E = \mathbf{A}\hat{\mathbf{x}}^E) = \mathcal{R}(\hat{\mathbf{y}}_{\mathbf{A}}) + \lambda_1^2 \frac{4d\|\mathbf{A}\|_2^2}{\frac{1}{k^2}\|\mathbf{A}_{\setminus k}\|_F^4} \quad (13)$$

This comes from a slight re-working of Theorem 3.1 of [Zou and Zhang \(2009\)](#). The bounds for the elastic net risk and $\mathcal{R}(\hat{\mathbf{y}}_{\mathbf{C}})$ are comparable when $\lambda_1^2 \approx \frac{\beta\epsilon}{k^2}\|\mathbf{A}_{\setminus k}\|_F^4 \frac{\mathcal{R}(\hat{\mathbf{y}}_{\mathbf{A}})}{4d\|\mathbf{A}\|_2^2}$.

Theorem 5. *Ridge Leverage Power-law Decay: Let $\mathbf{A} \in \mathbb{R}^{n \times d}$ be a matrix of at least rank k and $\bar{\tau}_i(\mathbf{A})$ be defined as in Eqn. 1. Furthermore, let the ridge leverage scores exhibit power-law decay in the sorted column index π_i ,*

$$\bar{\tau}_{\pi_i}(\mathbf{A}) = \pi_i^{-a} \bar{\tau}_{\pi_0}(\mathbf{A}) \quad a > 1. \quad (14)$$

Construct \mathbf{C} following the DRLS algorithm described in Sec. 2.1. The number of sample columns selected by DRLS is,

$$|\Theta| \leq \max \left(\left(\frac{4k}{\epsilon} \right)^{\frac{1}{a}} - 1, \left(\frac{4k}{(a-1)\epsilon} \right)^{\frac{1}{a-1}} - 1, k \right). \quad (15)$$

¹Thanks to Michael Mahoney for this point.

The concept of power-law decay behavior for leverage scores was introduced by [Papailiopoulos et al. \(2014\)](#) (Theorem 3) for rank- k subspace leverage scores. Our Theorem is an adaptation of [Papailiopoulos et al. \(2014\)](#)'s Theorem 3 for ridge leverage scores.

An obvious extension of Eqn. 7 is the following bound,

$$(1 - \epsilon) \mathbf{A} \mathbf{A}^T - \frac{\epsilon}{k} \|\mathbf{A}_{\setminus k}\|_F^2 \mathbf{I} \preceq \mathbf{C} \mathbf{C}^T \preceq (1 + \epsilon) \mathbf{A} \mathbf{A}^T + \frac{\epsilon}{k} \|\mathbf{A}_{\setminus k}\|_F^2 \mathbf{I}, \quad (16)$$

which also holds for \mathbf{C} selected by ridge leverage random sampling methods with $O(\frac{k}{\epsilon^2} \ln(\frac{k}{\delta}))$ weighted columns and failure probability δ [Cohen et al. \(2017\)](#). Thus, DRLS selects fewer columns with the same accuracy ϵ in Eqn. 16 for power-law decay in the ridge leverage scores when,

$$\max \left(\left(\frac{4k}{\epsilon} \right)^{\frac{1}{a}} - 1, \left(\frac{4k}{(a-1)\epsilon} \right)^{\frac{1}{a-1}} - 1, k \right) < C \frac{k}{\epsilon^2} \ln \left(\frac{k}{\delta} \right), \quad (17)$$

where C is an absolute constant. In particular, when $a \geq 2$, the number of columns deterministically sampled is $\mathcal{O}(k)$.²

4 Biological Data Illustration

We provide a biological data illustration of ridge leverage scores and ridge regression with multi-omic data from lower-grade glioma (LGG) tumor samples collected by the TCGA Research Network (<http://cancergenome.nih.gov/>). Diffuse lower-grade gliomas are infiltrative brain tumors that occur most frequently in the cerebral hemisphere of adults.

The data is publicly available and hosted by the Broad Institute's GDAC Firehose ([Broad Institute of MIT and Harvard, 2016](#)). We download the data using the *R* tool *TCGA2STAT* ([Wan et al., 2016](#)). *TCGA2STAT* imports the latest available version-stamped standardized Level 3 dataset on Firehose. The data collection and data platforms are discussed in detail in the original paper ([The Cancer Genome Atlas Research Network, 2015](#)).

We use the following multi-omic data types: mutations ($d = 4845$), DNA copy number (alteration ($d = 22618$) and variation ($d = 22618$)), messenger RNA (mRNA) expression ($d = 20501$), and microRNA expression ($d = 1046$). Methylation data is also available, but we omit it due to memory constraints. The mRNA and microRNA data is normalized. DNA copy number (variation and alteration) has an additional pre-processing step; the segmentation data reported by TCGA is turned into copy number using the *R* tool *CNtools* ([Zhang, 2015](#)) that is imbedded in *TCGA2STAT*. The mutation data is filtered based on status and variant classification and then aggregated at the gene level ([Wan et al., 2016](#)).

There are 280 tumor samples and $d = 71628$ multi-omic features in the downloaded dataset. We are interested in performing ridge regression with the biologically meaningful outcome variables relating to mutations of the "IDH1" and "IDH2" gene and deletions of the "1p/19q" chromosome arms ("code1"). These variables were shown to be predictive of favorable clinical outcomes and can be found in the supplemental tables ([The Cancer Genome Atlas Research Network, 2015](#)). We restrict to samples with these outcome variables (275 tumor samples), and we drop an additional sample ("TCGA-CS-4944") because it is an outlier with respect to the $k = 3$ SVD projection of the samples. This leaves a total of 274 tumor samples with outcome variables "IDH" (a mutation in either "IDH1" or "IDH2") and "code1" for the analysis.

Lastly, we drop all multi-omic features that have zero columns and greater than 10% missing data on the 274 tumor samples. We replace missing values with the mean of the column. This leaves a final multi-omic feature set of $d = 68522$ for the 274 tumor samples. Our final matrix $\mathbf{A} \in \mathbf{R}^{274 \times 68522}$ is column mean-centered.

4.1 Ridge leverage score sampling

Applying the DRLS algorithm with $k = 3, \epsilon = 0.1$ leads to $|\Theta| = 1512$, selecting approximately 0.02% of the total multi-omic features. Figure 1 shows the spectrum of eigenvalues of $\mathbf{A} \mathbf{A}^T$ for LGG. Figure 2 shows the relationship between the number of columns kept, $|\Theta|$, and $\tilde{\epsilon} = \sum_{i \notin \Theta} \bar{\tau}_i(\mathbf{A})$ for

²Thanks to Ahmed El Alaoui for this point.

the $k = 3$ ridge leverage scores. Figure 3 shows the power-law decay of the LGG $k = 3$ ridge leverage scores with sorted column index. The LGG multi-omic data shows that ridge leverage score power-law decay occurs in the wild. Figure 4 shows a histogram of the ratio of $\|\mathbf{C} - \mathbf{X}\mathbf{C}\|_F^2 / \|\mathbf{A} - \mathbf{X}\mathbf{A}\|_F^2$ for 1000 random rank- $k = 3$ orthogonal projections \mathbf{X} . The projections are chosen as the first 3 directions from an orthogonal basis randomly selected with respect to the Haar measure for the orthogonal group $O(n)$ (Mezzadri, 2006). Lastly, Figure 5 illustrates the $k = 3$ ridge leverage score regularization of the classical leverage score for the LGG multi-omic features.

4.2 Ridge regression with ridge leverage score sampling

We perform ridge regression with the appropriate regularization parameter for two biologically meaningful outcome variables; the first is whether either the "IDH1" or the "IDH2" gene is mutated and the second whether the "1p/19q" chromosome arms have deletions ("codel"). We encode the status of each event as ± 1 . Figures 6, 7, and 8 show the top three SVD projections for the tumor samples, colored by the combined status for "IDH" and "codel". No tumor samples have the "1p/19q" codeletion and no "IDH" mutation. Visual inspection of the SVD plot confirms that this is a reasonable regression problem for "IDH" and a difficult regression problem for "codel"; also, logistic regression would be more natural for binary outcomes. We proceed anyway, since our objective is to compare ridge regression with all of the features \mathbf{A} to ridge regression the DRLS subset \mathbf{C} on realistic biological data. Figures 9 and 10 confirm that the ridge regression fits are close $(\hat{\mathbf{y}}_{\mathbf{A}} - \hat{\mathbf{y}}_{\mathbf{C}})$ for all the tumor samples. Figures 11 and 12 confirm that the ridge regression coefficients are close $(\hat{\mathbf{x}}_{\mathbf{A}} - \hat{\mathbf{x}}_{\mathbf{C}})$ for all the tumor samples. Figure 13 and 14 illustrate the overall performance of ridge regression for these two outcome variables.

Lastly, we simulate 274 samples according to the linear model (Eqn. 4), where $\mathbf{y}^* = \mathbf{A}\mathbf{x}^*$, the coefficients $\mathbf{x}^* \sim \mathcal{N}(0, \mathbf{I})$, and \mathbf{A} is the LGG multi-omic feature matrix. We choose $\sigma^2 = \{10^{-3}, 1, 10^3\}$. We perform ridge regression with \mathbf{A} and then again with \mathbf{C} in accordance with Theorem 4. We calculate the risks $\mathcal{R}(\hat{\mathbf{y}}_{\mathbf{A}})$ and $\mathcal{R}(\hat{\mathbf{y}}_{\mathbf{C}})$ and find that Theorem 4 is not violated. Table 1 shows the risk ratios $\mathcal{R}(\hat{\mathbf{y}}_{\mathbf{C}})/\mathcal{R}(\hat{\mathbf{y}}_{\mathbf{A}})$ along with other relevant ratios for the ridge leverage scores.

Table 1: Ridge leverage score ratios for $k = 3, \epsilon = 0.1$ for LGG tumor multi-omic data. The ratios are near one, as expected. Ridge regression risk ratio for data simulated from the LGG multi-omic feature matrix and Eqn. 4.

ave($\Sigma_{\mathbf{C}}^2/\Sigma^2$)	$\ \mathbf{C}_{\setminus k}\ _F^2/\ \mathbf{A}_{\setminus k}\ _F^2$	ave($\bar{\Sigma}^2/\bar{\Sigma}_{\mathbf{C}}^2$)	σ^2	$\mathcal{R}(\hat{\mathbf{y}}_{\mathbf{C}})/\mathcal{R}(\hat{\mathbf{y}}_{\mathbf{A}})$
0.85	0.97	1.03	10^{-3}	0.99
			10^0	0.99
			10^3	0.99

5 Proofs

5.1 Brief Review

See Horn and Johnson (2013) for a linear algebra review. A square complex matrix \mathbf{F} is *Hermitian* if $\mathbf{F} = \mathbf{F}^\dagger$. Symmetric positive semi-definite (S.P.S.D) matrices are Hermitian matrices. The set of $n \times n$ Hermitian matrices is a real linear space. As such, it is possible to define a *partial ordering* (also called a Loewner partial ordering, denoted by \preceq) on the real linear space. One matrix is "greater" than another if their difference lies in the closed convex cone of S.P.S.D. matrices. Let \mathbf{F}, \mathbf{G} be Hermitian and the same size, and \mathbf{x} a complex vector of compatible dimension. Then,

$$\mathbf{F} \preceq \mathbf{G} \iff \mathbf{x}^\dagger \mathbf{F} \mathbf{x} \leq \mathbf{x}^\dagger \mathbf{G} \mathbf{x} \quad \forall \mathbf{x} \neq \mathbf{0}. \quad (18)$$

If \mathbf{F} is Hermitian with smallest and largest eigenvalues $\lambda_{\min}(\mathbf{F}), \lambda_{\max}(\mathbf{F})$, respectively, then,

$$\lambda_{\min}(\mathbf{F}) \mathbf{I} \preceq \mathbf{F} \preceq \lambda_{\max}(\mathbf{F}) \mathbf{I}. \quad (19)$$

Let \mathbf{F}, \mathbf{G} be Hermitian and the same size, and let \mathbf{H} be any complex rectangular matrix of compatible dimension. The *conjugation rule* is,

$$\text{If } \mathbf{F} \preceq \mathbf{G}, \text{ then } \mathbf{H} \mathbf{F} \mathbf{H}^\dagger \preceq \mathbf{H} \mathbf{G} \mathbf{H}^\dagger. \quad (20)$$

In addition, let $\lambda_i(\mathbf{F})$ and $\lambda_i(\mathbf{G})$ be the non-decreasingly ordered eigenvalues of \mathbf{F}, \mathbf{G} . Then,

$$\text{If } \mathbf{F} \preceq \mathbf{G}, \text{ then } \forall i, \lambda_i(\mathbf{F}) \leq \lambda_i(\mathbf{G}). \quad (21)$$

Since the trace of a matrix \mathbf{F} is the sum of its eigenvalues, $\text{tr } \mathbf{F} = \sum_i \lambda_i(\mathbf{F})$, and the Loewner ordering implies the ordering of eigenvalues (Eqn. 21), the Loewner ordering also implies the ordering of their sum,

$$\text{If } \mathbf{F} \preceq \mathbf{G}, \text{ then } \text{tr } \mathbf{F} \leq \text{tr } \mathbf{G}. \quad (22)$$

5.2 Proof of ridge leverage score sum

The sum of ridge leverage scores is,

$$\begin{aligned} \sum_{i=1}^d \bar{\tau}_i(\mathbf{A}) &= \text{tr } \mathbf{A}^T \left(\mathbf{A} \mathbf{A}^T + \frac{1}{k} \|\mathbf{A} - \mathbf{A}_k\|_F^2 \mathbf{I} \right)^+ \mathbf{A} \\ &= \text{tr } \mathbf{A}^T \mathbf{U} \bar{\Sigma}^{-2} \mathbf{U}^T \mathbf{A} = \text{tr } \bar{\Sigma}^{-2} \Sigma^2, \end{aligned} \quad (23)$$

where $\bar{\Sigma}$ is diagonal and $\bar{\Sigma}_{i,i}^2 = \Sigma_{i,i}^2 + \frac{1}{k} \|\mathbf{A}_{\setminus k}\|_F^2$. We split the sum into two parts,

$$\begin{aligned} &= \sum_{i=1}^k \frac{\Sigma_{i,i}^2}{\Sigma_{i,i}^2 + \frac{1}{k} \|\mathbf{A}_{\setminus k}\|_F^2} + \sum_{i=k+1}^n \frac{\Sigma_{i,i}^2}{\Sigma_{i,i}^2 + \frac{1}{k} \|\mathbf{A}_{\setminus k}\|_F^2} \\ &\leq \sum_{i=1}^k \frac{\Sigma_{i,i}^2}{\Sigma_{i,i}^2} + \sum_{i=k+1}^n \frac{\Sigma_{i,i}^2}{\frac{1}{k} \|\mathbf{A}_{\setminus k}\|_F^2} = k + k. \end{aligned} \quad (24)$$

This proof is due to Cohen et al. (2017).

5.3 Proof of Theorem 1

The upper bound in Eqn. 7 in Theorem 1 follows from the fact that $\mathbb{0} \preceq \mathbf{I} - \mathbf{S} \mathbf{S}^T$ and the conjugation rule (Eqn. 20),

$$\mathbb{0} \preceq \mathbf{A}(\mathbf{I} - \mathbf{S} \mathbf{S}^T) \mathbf{A}^T = \mathbf{A} \mathbf{A}^T - \mathbf{C} \mathbf{C}^T. \quad (25)$$

This upper bound is true for any column selection of \mathbf{A} .

For the lower bound in Eqn. 7, consider the quantity,

$$\mathbf{Y} = \bar{\Sigma}^{-1} \mathbf{U}^T \mathbf{A}(\mathbf{I} - \mathbf{S} \mathbf{S}^T) \mathbf{A}^T \mathbf{U} \bar{\Sigma}^{-1} = \bar{\Sigma}^{-1} \Sigma \mathbf{V}^T (\mathbf{I} - \mathbf{S} \mathbf{S}^T) \mathbf{V} \Sigma \bar{\Sigma}^{-1}.$$

By the conjugation rule (Eqn. 20) on Eqn. 25, $\mathbb{0} \preceq \mathbf{Y}$, so \mathbf{Y} is S.P.S.D. By the construction of DRLS (Eqn. 6) $\text{tr } \mathbf{Y} = \sum_{i \notin \Theta} \sum_{l=1}^n \bar{\Sigma}_{l,l}^{-2} \Sigma_{l,l}^2 V_{il}^2 = \tilde{\epsilon} < \epsilon$, and because \mathbf{Y} is S.P.S.D., $\lambda_{\max}(\mathbf{Y}) \leq \text{tr } \mathbf{Y}$. By Eqn. 19 and the previous facts, $\mathbf{Y} \preceq \lambda_{\max}(\mathbf{Y}) \mathbf{I} \preceq \epsilon \mathbf{I}$. As a result of the conjugation rule applied to this upper bound,

$$\mathbf{U} \bar{\Sigma} \mathbf{Y} \bar{\Sigma} \mathbf{U}^T = \mathbf{A} \mathbf{A}^T - \mathbf{C} \mathbf{C}^T \preceq \epsilon \mathbf{U} \bar{\Sigma}^2 \mathbf{U}^T = \epsilon \left(\mathbf{A} \mathbf{A}^T + \frac{1}{k} \|\mathbf{A}_{\setminus k}\|_F^2 \mathbf{I} \right),$$

and rearrangement leads to the lower bound of Eqn. 7.

5.4 Proof of Theorem 2

To prove Eqn. 8, we will use the following lemma.

Lemma 2. (Boutsidis et al. (2011) Lemma 3.1, Eqn. 3.2, specialized to the Frobenius norm): Consider $\mathbf{A} = \mathbf{A} \mathbf{Z} \mathbf{Z}^T + \mathbf{E} \in \mathbb{R}^{n \times d}$, where $\mathbf{Z} \in \mathbb{R}^{n \times k}$ and $\mathbf{Z}^T \mathbf{Z} = \mathbf{I}_k$. Let $\mathbf{S} \in \mathbb{R}^{n \times |\Theta|}$ ($k \leq |\Theta|$) be any matrix such that $\text{rank}(\mathbf{Z}^T \mathbf{S}) = k$, and let $\mathbf{C} = \mathbf{A} \mathbf{S}$. Then,

$$\|\mathbf{A} - \mathbf{C} \mathbf{C}^+ \mathbf{A}\|_F^2 \leq \|\mathbf{A} - \Pi_{\mathbf{C},k}^F(\mathbf{A})\|_F^2 \leq \|\mathbf{E}\|_F^2 \|\mathbf{S}(\mathbf{Z}^T \mathbf{S})^+\|_2^2, \quad (26)$$

where $\Pi_{\mathbf{C},k}^F(\mathbf{A}) = (\mathbf{C} \mathbf{C}^+ \mathbf{A})_k$ is the best rank- k approximation to \mathbf{A} in the column space of \mathbf{C} with the respect to the Frobenius norm.

We'll use a slightly relaxed version of Lemma 2,

$$\|\mathbf{A} - \mathbf{CC}^+ A\|_F^2 \leq \|\mathbf{A} - \Pi_{\mathbf{C},k}^F(\mathbf{A})\|_F^2 \leq \|\mathbf{E}\|_F^2 \|\mathbf{S}\|_2^2 \|(\mathbf{Z}^T \mathbf{S})^+\|_2^2. \quad (27)$$

Choosing $\mathbf{Z} = \mathbf{V}_k$, and noting that $\|\mathbf{S}\|_2^2 = 1$, we have

$$\|\mathbf{A} - \mathbf{CC}^+ A\|_F^2 \leq \|\mathbf{A} - \Pi_{\mathbf{C},k}^F(\mathbf{A})\|_F^2 \leq \|\mathbf{A}_{\setminus k}\|_F^2 \|(\mathbf{V}_k^T \mathbf{S})^+\|_2^2. \quad (28)$$

It remains to calculate $\|(\mathbf{V}_k^T \mathbf{S})^+\|_2^2 = \sigma_k^{-2}(\mathbf{V}_k \mathbf{S} \mathbf{S}^T \mathbf{V}_k^T)$, where $k \leq \text{rank}(\mathbf{A}) = r$. As a consequence of the conjugation rule (Eqn. 20) applied to Eqn. 7 with pre- (post-)multiplication by $\Sigma_k^{-1} \mathbf{U}_k^T$ ($\mathbf{U}_k \Sigma_k^{-1}$), we have,

$$(1 - \epsilon) \mathbf{I}_k - \frac{\epsilon}{k} \|\mathbf{A}_{\setminus k}\|_F^2 \Sigma_k^{-2} \preceq \mathbf{V}_k \mathbf{S} \mathbf{S}^T \mathbf{V}_k^T \quad (29)$$

From Eqn. 29, the k^{th} eigenvalue $\sigma_k^2(\mathbf{V}_k \mathbf{S} \mathbf{S}^T \mathbf{V}_k^T)$ obeys,

$$(1 - 2\epsilon) \leq \sigma_k^2(\mathbf{V}_k \mathbf{S} \mathbf{S}^T \mathbf{V}_k^T), \quad (30)$$

after using the fact that $\frac{1}{k} \|\mathbf{A}_{\setminus k}\|_F^2 \Sigma_k^{-2} \leq 1$ (by definition). Eqn. 30 shows that, for $0 < \epsilon < \frac{1}{2}$, $\text{rank}(\mathbf{V}_k^T \mathbf{S}) = k$. Combining Eqn. 28 and Eqn. 30 gives Eqn. 8. This proof illustrates the power of the spectral bound (Eqn. 7), since the column subset selection bound (Eqn. 8) is a direct consequence of Eqn. 7.

5.5 Proof of Theorem 3

It will be convenient to define the projection matrix $\mathbf{Y} = \mathbf{I} - \mathbf{X}$. Then the upper bound in Eqn. 9 follows directly from upper spectral bound (Eqn. 25), the conjugation rule (Eqn. 20), and the trace rule (Eqn. 22).

The lower projection-cost preservation bound is considerably more involved to prove, and also relies primarily on the spectral bound (Eqn. 7) and facts from linear algebra. Our proof is nearly identical to the proof of Cohen et al. (2017)'s Theorem 4, with only one large deviation and several small differences in constants. We include the full proof for completeness, and point out the major difference.

We split \mathbf{AA}^T and \mathbf{CC}^T into their projections on the top m "head" singular vectors and the remaining "tail" singular vectors. Choose m such that $\Sigma_{m,m}$ is the smallest singular value that obeys $\Sigma_{m,m}^2 \geq \frac{1}{k} \|\mathbf{A}_{\setminus k}\|_F^2$. Let $\mathbf{P}_m = \mathbf{U}_m \mathbf{U}_m^T$ and $\mathbf{P}_{\setminus m} = \mathbf{U}_{\setminus m} \mathbf{U}_{\setminus m}^T$ be projection matrices. Note that,

$$\begin{aligned} \text{tr}(\mathbf{Y} \mathbf{AA}^T \mathbf{Y}) &= \text{tr}(\mathbf{Y} \mathbf{A}_m \mathbf{A}_m^T \mathbf{Y}) + \text{tr}(\mathbf{Y} \mathbf{A}_{\setminus m} \mathbf{A}_{\setminus m}^T \mathbf{Y}) \\ \text{tr}(\mathbf{Y} \mathbf{CC}^T \mathbf{Y}) &= \text{tr}(\mathbf{Y} \mathbf{P}_m \mathbf{CC}^T \mathbf{P}_m^T \mathbf{Y}) + \text{tr}(\mathbf{Y} \mathbf{P}_{\setminus m} \mathbf{CC}^T \mathbf{P}_{\setminus m}^T \mathbf{Y}) \\ &\quad + 2\text{tr}(\mathbf{Y} \mathbf{P}_m \mathbf{CC}^T \mathbf{P}_{\setminus m}^T \mathbf{Y}). \end{aligned} \quad (31)$$

5.5.1 Head terms

First we bound the terms involving only \mathbf{P}_m . Consider Eqn. 7 and the vector $\mathbf{y} = \mathbf{P}_m \mathbf{x}$ for any vector \mathbf{x} . Eqn. 7 gives,

$$\begin{aligned} (1 - \epsilon) \mathbf{x}^T \mathbf{P}_m \mathbf{AA}^T \mathbf{P}_m \mathbf{x} - \frac{\epsilon}{k} \|\mathbf{A}_{\setminus k}\|_F^2 \mathbf{y}^T \mathbf{y} &\leq \mathbf{y}^T \mathbf{CC}^T \mathbf{y} \\ (1 - 2\epsilon) \mathbf{x}^T \mathbf{P}_m \mathbf{AA}^T \mathbf{P}_m \mathbf{x} &\leq \mathbf{x}^T \mathbf{P}_m \mathbf{CC}^T \mathbf{P}_m \mathbf{x}, \end{aligned}$$

because by the artful definition of m , $\mathbf{x}^T \mathbf{P}_m \mathbf{AA}^T \mathbf{P}_m \mathbf{x} \geq \frac{1}{k} \|\mathbf{A}_{\setminus k}\|_F^2 \mathbf{y}^T \mathbf{y}$. Therefore we have,

$$(1 - 2\epsilon) \mathbf{P}_m \mathbf{AA}^T \mathbf{P}_m \preceq \mathbf{P}_m \mathbf{CC}^T \mathbf{P}_m, \quad (32)$$

and finally,

$$(1 - 2\epsilon) \text{tr}(\mathbf{Y} \mathbf{A}_m \mathbf{A}_m^T \mathbf{Y}) \leq \text{tr}(\mathbf{Y} \mathbf{P}_m \mathbf{CC}^T \mathbf{P}_m \mathbf{Y}). \quad (33)$$

5.5.2 Tail terms

To bound the lower singular directions of \mathbf{A} , we decompose $\text{tr}(\mathbf{Y}\mathbf{A}_{\setminus m}\mathbf{A}_{\setminus m}^T\mathbf{Y})$ further as,

$$\text{tr}(\mathbf{Y}\mathbf{A}_{\setminus m}\mathbf{A}_{\setminus m}^T\mathbf{Y}) = \text{tr}(\mathbf{A}_{\setminus m}\mathbf{A}_{\setminus m}^T) - \text{tr}(\mathbf{X}\mathbf{A}_{\setminus m}\mathbf{A}_{\setminus m}^T\mathbf{X}), \quad (34)$$

and analogously for \mathbf{C} .

The upper spectral bound (Eqn. 25), the conjugation rule (Eqn. 20) gives,

$$\mathbf{P}_{\setminus m}\mathbf{C}\mathbf{C}^T\mathbf{P}_{\setminus m} \preceq \mathbf{P}_{\setminus m}\mathbf{A}\mathbf{A}^T\mathbf{P}_{\setminus m}, \quad (35)$$

The conjugation rule (Eqn. 20), and the trace rule (Eqn. 22) give,

$$\text{tr}(\mathbf{X}\mathbf{P}_{\setminus m}\mathbf{C}\mathbf{C}^T\mathbf{P}_{\setminus m}\mathbf{X}) \leq \text{tr}(\mathbf{X}\mathbf{P}_{\setminus m}\mathbf{A}\mathbf{A}^T\mathbf{P}_{\setminus m}\mathbf{X}). \quad (36)$$

Next we consider $\|\mathbf{P}_{\setminus m}\mathbf{A}\|_F^2 - \|\mathbf{P}_{\setminus m}\mathbf{C}\|_F^2$. In Cohen et al. (2017)'s proof, a scalar Chernoff bound is used for $\|\mathbf{P}_{\setminus m}\mathbf{A}\|_F^2 - \|\mathbf{P}_{\setminus m}\mathbf{C}\|_F^2$ (Cohen et al. (2017) Section 4.3, Eqn. 17). Since our matrix \mathbf{C} is constructed deterministically, we will prove and substitute the following bound (Eqn. 37),

$$0 \leq \|\mathbf{P}_{\setminus m}\mathbf{A}\|_F^2 - \|\mathbf{P}_{\setminus m}\mathbf{C}\|_F^2 \leq 2\epsilon\|\mathbf{A}_{\setminus k}\|_F^2. \quad (37)$$

for the scalar Chernoff bound.

To prove Eqn. 37, we first note the lower bound follows directly from upper spectral bound (Eqn. 25), the conjugation rule (Eqn. 20), and the trace rule (Eqn. 22). To prove the upper bound, we rewrite the difference in Frobenius norms as a difference in sums over column norms:

$$\begin{aligned} \|\mathbf{P}_{\setminus m}\mathbf{A}\|_F^2 - \|\mathbf{P}_{\setminus m}\mathbf{C}\|_F^2 &= \sum_{j \notin \Theta} \|\mathbf{P}_{\setminus m}\mathbf{a}_j\|_F^2 = \sum_{j \notin \Theta} \text{tr} \mathbf{a}_j^T \mathbf{P}_{\setminus m} \mathbf{P}_{\setminus m} \mathbf{a}_j \\ &\leq \frac{2}{k} \|\mathbf{A}_{\setminus k}\|_F^2 \sum_{j \notin \Theta} \text{tr} \mathbf{a}_j^T \mathbf{P}_{\setminus m} \mathbf{U}_{\setminus m} \bar{\Sigma}^{-2} \mathbf{U}_{\setminus m}^T \mathbf{P}_{\setminus m} \mathbf{a}_j \\ &\leq \frac{2}{k} \|\mathbf{A}_{\setminus k}\|_F^2 \sum_{j \notin \Theta} \text{tr} \mathbf{a}_j^T \mathbf{U} \bar{\Sigma}^{-2} \mathbf{U} \mathbf{a}_j \\ &= \frac{2\tilde{\epsilon}}{k} \|\mathbf{A}_{\setminus k}\|_F^2 \leq 2\epsilon \|\mathbf{A}_{\setminus k}\|_F^2. \end{aligned} \quad (38)$$

The first inequality follows from the fact that $\bar{\Sigma}_{i,i}^2 = \Sigma_{i,i}^2 + \frac{1}{k}\|\mathbf{A}_{\setminus k}\|_F^2 \leq \frac{2}{k}\|\mathbf{A}_{\setminus k}\|_F^2$ for $i \geq m$. As a result, $\mathbf{P}_{\setminus m} \preceq \frac{2}{k}\|\mathbf{A}_{\setminus k}\|_F^2 \mathbf{U}_{\setminus m} \bar{\Sigma}^{-2} \mathbf{U}_{\setminus m}^T$.

Combining the upper bound of Eqn. 37 with Eqn. 36 gives,

$$\text{tr}(\mathbf{Y}\mathbf{A}_{\setminus m}\mathbf{A}_{\setminus m}^T\mathbf{Y}) - 2\epsilon\|\mathbf{A}_{\setminus k}\|_F^2 \leq \text{tr}(\mathbf{Y}\mathbf{P}_{\setminus m}\mathbf{C}\mathbf{C}^T\mathbf{P}_{\setminus m}\mathbf{Y}). \quad (39)$$

5.5.3 Cross terms

Finally, we show $\text{tr}(\mathbf{Y}\mathbf{P}_{\setminus m}\mathbf{C}\mathbf{C}^T\mathbf{P}_{\setminus m}\mathbf{Y})$ is small. We rewrite it as,

$$\text{tr}(\mathbf{Y}\mathbf{P}_{\setminus m}\mathbf{C}\mathbf{C}^T\mathbf{P}_{\setminus m}\mathbf{Y}) = \text{tr}(\mathbf{Y}\mathbf{A}\mathbf{A}^T(\mathbf{A}\mathbf{A}^T)^+\mathbf{P}_{\setminus m}\mathbf{C}\mathbf{C}^T\mathbf{P}_{\setminus m}\mathbf{Y}), \quad (40)$$

using the cyclic property of the trace and the fact that $\mathbf{P}_{\setminus m}\mathbf{C}\mathbf{C}^T\mathbf{P}_{\setminus m}^T$ is in \mathbf{A} 's column span. Because $(\mathbf{A}\mathbf{A}^T)^+$ is semi-positive definite and defines a semi-inner product, we can use the Cauchy-Schwarz inequality,

$$\begin{aligned} |\text{tr}(\mathbf{Y}\mathbf{A}\mathbf{A}^T(\mathbf{A}\mathbf{A}^T)^+\mathbf{P}_{\setminus m}\mathbf{C}\mathbf{C}^T\mathbf{P}_{\setminus m}\mathbf{Y})| &\leq \left(\text{tr}(\mathbf{Y}\mathbf{A}\mathbf{A}^T(\mathbf{A}\mathbf{A}^T)^+\mathbf{A}\mathbf{A}^T\mathbf{Y}) \right)^{\frac{1}{2}} \\ &\quad \times \left(\text{tr}(\mathbf{P}_{\setminus m}\mathbf{C}\mathbf{C}^T\mathbf{P}_{\setminus m}^T(\mathbf{A}\mathbf{A}^T)^+\mathbf{P}_{\setminus m}\mathbf{C}\mathbf{C}^T\mathbf{P}_{\setminus m}^T) \right)^{\frac{1}{2}} \\ &= \left(\text{tr}(\mathbf{Y}\mathbf{A}\mathbf{A}^T\mathbf{Y}) \right)^{\frac{1}{2}} \|\mathbf{P}_{\setminus m}\mathbf{C}\mathbf{C}^T\mathbf{U}_m \Sigma_m^{-1}\|_F. \end{aligned}$$

(41)

The square of the second term decomposes as,

$$\|\mathbf{P}_{\setminus m} \mathbf{CC}^T \mathbf{U}_m \Sigma_m^{-1}\|_F^2 = \sum_{i=1}^m \|\mathbf{P}_{\setminus m} \mathbf{CC}^T \mathbf{u}_i\|_2^2 \Sigma_{i,i}^{-2}, \quad (42)$$

which is small for every i . To show this, we define two convenient vectors. The first is the unit vector $\mathbf{p}_i = \frac{1}{\|\mathbf{P}_{\setminus m} \mathbf{CC}^T \mathbf{u}_i\|_2} \mathbf{P}_{\setminus m} \mathbf{CC}^T \mathbf{u}_i$. Note that $\mathbf{p}_i^T \mathbf{u}_i = 0$. This is convenient because $(\mathbf{p}_i^T \mathbf{CC}^T \mathbf{u}_i)^2 = \|\mathbf{P}_{\setminus m} \mathbf{CC}^T \mathbf{u}_i\|_2^2$. The second vector is $\mathbf{m} = \Sigma_{i,i}^{-1} \mathbf{u}_i + \frac{\sqrt{k}}{\|\mathbf{A}_{\setminus k}\|_F} \mathbf{p}_i$. From Eqn. 25,

$$\begin{aligned} \mathbf{m}^T \mathbf{CC}^T \mathbf{m} &\leq \mathbf{m}^T \mathbf{AA}^T \mathbf{m} \\ \Sigma_{i,i}^{-2} \mathbf{u}_i^T \mathbf{CC}^T \mathbf{u}_i + \frac{k}{\|\mathbf{A}_{\setminus k}\|_F^2} \mathbf{p}_i^T \mathbf{CC}^T \mathbf{p}_i + \frac{2\sqrt{k}}{\Sigma_{i,i} \|\mathbf{A}_{\setminus k}\|_F} \mathbf{p}_i^T \mathbf{CC}^T \mathbf{u}_i &\leq \\ \Sigma_{i,i}^{-2} \mathbf{u}_i^T \mathbf{AA}^T \mathbf{u}_i + \frac{k}{\|\mathbf{A}_{\setminus k}\|_F^2} \mathbf{p}_i^T \mathbf{AA}^T \mathbf{p}_i &= 1 + \frac{k}{\|\mathbf{A}_{\setminus k}\|_F^2} \mathbf{p}_i^T \mathbf{AA}^T \mathbf{p}_i. \end{aligned} \quad (43)$$

From Eqn. 32, we have,

$$(1 - 2\epsilon) \Sigma_{i,i} = (1 - 2\epsilon) \mathbf{u}_i \mathbf{AA}^T \mathbf{u}_i \leq \mathbf{u}_i \mathbf{CC}^T \mathbf{u}_i. \quad (44)$$

From Eqn. 35, we have,

$$\mathbf{p}_i \mathbf{CC}^T \mathbf{p}_i \leq \mathbf{p}_i \mathbf{AA}^T \mathbf{p}_i. \quad (45)$$

Using these facts, Eqn. 43 becomes,

$$\begin{aligned} (1 - 2\epsilon) + \frac{k}{\|\mathbf{A}_{\setminus k}\|_F^2} \mathbf{p}_i^T \mathbf{CC}^T \mathbf{p}_i + \frac{2\sqrt{k}}{\Sigma_{i,i} \|\mathbf{A}_{\setminus k}\|_F} \mathbf{p}_i^T \mathbf{CC}^T \mathbf{u}_i &\leq \\ 1 + \frac{k}{\|\mathbf{A}_{\setminus k}\|_F^2} \mathbf{p}_i^T \mathbf{CC}^T \mathbf{p}_i & \\ (\mathbf{p}_i^T \mathbf{CC}^T \mathbf{u}_i)^2 &\leq \epsilon^2 \frac{\Sigma_{i,i}^2 \|\mathbf{A}_{\setminus k}\|_F^2}{k}. \end{aligned} \quad (46)$$

Returning to Eqn. 42 with this, we have

$$\|\mathbf{P}_{\setminus m} \mathbf{CC}^T \mathbf{U}_m \Sigma_m^{-1}\|_F^2 \leq \sum_{i=1}^m \epsilon^2 \frac{\|\mathbf{A}_{\setminus k}\|_F^2}{k} \leq 2\epsilon^2 \|\mathbf{A}_{\setminus k}\|_F^2. \quad (47)$$

The factor of 2 comes from the fact that $m \leq 2k$. After recalling that the Eckart-Young-Mirsky theorem (Eckart and Young, 1936) gives $\|\mathbf{A}_{\setminus k}\|_F^2 \leq \text{tr}(\mathbf{Y} \mathbf{AA}^T \mathbf{Y})$, we have for Eqn. 41,

$$|\text{tr}(\mathbf{Y} \mathbf{AA}^T (\mathbf{AA}^T)^+ \mathbf{P}_m \mathbf{CC}^T \mathbf{P}_{\setminus m}^T)| \leq \sqrt{2}\epsilon \text{tr}(\mathbf{Y} \mathbf{AA}^T \mathbf{Y}). \quad (48)$$

Combining Eqn. 31, Eqn. 33, Eqn. 39, Eqn. 48 leads to,

$$\begin{aligned} (1 - 2\epsilon) \text{tr}(\mathbf{Y} \mathbf{A}_m \mathbf{A}_m^T \mathbf{Y}) + \text{tr}(\mathbf{Y} \mathbf{A}_{\setminus m} \mathbf{A}_{\setminus m}^T \mathbf{Y}) - 2\epsilon \|\mathbf{A}_{\setminus k}\|_F^2 \\ - 2\sqrt{2}\epsilon \text{tr}(\mathbf{Y} \mathbf{AA}^T \mathbf{Y}) \leq \text{tr}(\mathbf{Y} \mathbf{CC}^T \mathbf{Y}). \end{aligned} \quad (49)$$

Again applying $\|\mathbf{A}_{\setminus k}\|_F^2 \leq \text{tr}(\mathbf{Y} \mathbf{AA}^T \mathbf{Y})$ and subtracting an extra $0 \leq 2\epsilon \text{tr}(\mathbf{Y} \mathbf{A}_{\setminus m} \mathbf{A}_{\setminus m}^T \mathbf{Y})$ from the lefthand side gives,

$$(1 - 2(2 + \sqrt{2})\epsilon) \text{tr}(\mathbf{Y} \mathbf{AA}^T \mathbf{Y}) \leq \text{tr}(\mathbf{Y} \mathbf{CC}^T \mathbf{Y}), \quad (50)$$

proving Theorem 3.

5.6 Proof of Lemma 1

Let the SVD of \mathbf{C} be $\mathbf{C} = \mathbf{W}\Sigma_{\mathbf{C}}\mathbf{Z}^T$. Set $\mathbf{X} = \mathbf{W}_k\mathbf{W}_k^T$. From the left-hand side of Eqn. 9 and the Eckart-Young-Mirsky theorem (Eckart and Young, 1936),

$$(1 - \alpha\epsilon)\|\mathbf{A}_{\setminus k}\|_F^2 \leq (1 - \alpha\epsilon)\|\mathbf{A} - \mathbf{X}\mathbf{A}\|_F^2 \leq \|\mathbf{C}_{\setminus k}\|_F^2. \quad (51)$$

Similarly, set $\mathbf{X} = \mathbf{U}_k\mathbf{U}_k^T$. From the right-hand side of Eqn. 9,

$$\|\mathbf{C}_{\setminus k}\|_F^2 \leq \|\mathbf{C} - \mathbf{X}\mathbf{C}\|_F^2 \leq \|\mathbf{A}_{\setminus k}\|_F^2. \quad (52)$$

This means that,

$$(1 - \alpha\epsilon)\|\mathbf{A}_{\setminus k}\|_F^2 \mathbf{I} \preceq \|\mathbf{C}_{\setminus k}\|_F^2 \mathbf{I} \preceq \|\mathbf{A}_{\setminus k}\|_F^2 \mathbf{I}. \quad (53)$$

Adding $1/k$ times Eqn. 53 to Eqn. 7 gives,

$$(1 - \epsilon)\mathbf{K}(\mathbf{A})^{-1} - \frac{\alpha\epsilon}{k}\|\mathbf{A}_{\setminus k}\|_F^2 \mathbf{I} \preceq \mathbf{K}(\mathbf{C})^{-1} \preceq \mathbf{K}(\mathbf{A})^{-1}. \quad (54)$$

Noting that we can subtract $\alpha\epsilon\mathbf{A}\mathbf{A}^T$ from the left-most side of Eqn. 54 and that all of the matrices are invertible gives the lemma.

5.7 Proof of Theorem 4

For ridge regression with matrix \mathbf{A} and estimator $\hat{\mathbf{y}} = \mathbf{A}\hat{\mathbf{x}}$, the statistical risk of the estimator $\mathcal{R}(\hat{\mathbf{y}}_{\mathbf{A}})$ is,

$$\mathcal{R}(\hat{\mathbf{y}}_{\mathbf{A}}) = \frac{1}{n}\mathbb{E}_{\xi} \left[\left\| \mathbf{A} \left(\mathbf{A}^T \mathbf{A} + \frac{\|\mathbf{A}_{\setminus k}\|_F^2}{k} \mathbf{I} \right)^{-1} \mathbf{A}^T (\mathbf{y}^* + \sigma^2 \xi) - \mathbf{y}^* \right\|_2^2 \right]. \quad (55)$$

Decomposing into bias and variance terms, taking the expectation, and using the Woodbury matrix inversion formula gives,

$$\begin{aligned} \mathcal{R}(\hat{\mathbf{y}}_{\mathbf{A}}) &= \frac{1}{n} \left\| \left(\mathbf{A} \left(\mathbf{A}^T \mathbf{A} + \frac{\|\mathbf{A}_{\setminus k}\|_F^2}{k} \mathbf{I} \right)^{-1} \mathbf{A}^T - \mathbf{I} \right) \mathbf{y}^* \right\|_2^2 \\ &+ \frac{\sigma^2}{n} \text{tr} \left(\left(\mathbf{A} \left(\mathbf{A}^T \mathbf{A} + \frac{\|\mathbf{A}_{\setminus k}\|_F^2}{k} \mathbf{I} \right)^{-1} \mathbf{A}^T \right)^2 \right) \\ &= \frac{\|\mathbf{A}_{\setminus k}\|_F^4}{nk^2} \left\| \left(\mathbf{A} \mathbf{A}^T + \frac{\|\mathbf{A}_{\setminus k}\|_F^2}{k} \mathbf{I} \right)^{-1} \mathbf{y}^* \right\|_2^2 \\ &+ \frac{\sigma^2}{n} \text{tr} \left(\left(\mathbf{A} \left(\mathbf{A}^T \mathbf{A} + \frac{\|\mathbf{A}_{\setminus k}\|_F^2}{k} \mathbf{I} \right)^{-1} \mathbf{A}^T \right)^2 \right) \\ &\equiv \text{bias}(\mathbf{A})^2 + \text{variance}(\mathbf{A}). \end{aligned} \quad (56)$$

We begin with the variance term. Using the SVD of \mathbf{A} on the variance term gives,

$$\text{variance}(\mathbf{A}) = \frac{\sigma^2}{n} \text{tr} \left(\Sigma^4 \bar{\Sigma}^{-4} \right). \quad (57)$$

As a consequence of Eqn. 21 and Eqn. 7,

$$\Sigma_{\mathbf{C}}^2 \preceq \Sigma^2. \quad (58)$$

As a consequence of Eqn. 21 and Eqn. 10,

$$\bar{\Sigma}^{-2} \preceq \bar{\Sigma}_{\mathbf{C}}^{-2} \preceq \frac{1}{1 - (\alpha + 1)\epsilon} \bar{\Sigma}^{-2}, \quad (59)$$

where $\bar{\Sigma}_{\mathbf{C}}^2 = \Sigma_{\mathbf{C}}^2 + \frac{1}{k}\|\mathbf{C}_{\setminus k}\|_F^2 \mathbf{I}$. Because the matrices in Eqn. 58 and Eqn. 59 are diagonal and (semi-) positive definite, the relationships can be squared. Finally, because the product of $\frac{1}{(1 - (\alpha + 1)\epsilon)^2} \Sigma^4 \bar{\Sigma}^{-4}$ is bigger or equal to the product of $\Sigma_{\mathbf{C}}^4 \bar{\Sigma}_{\mathbf{C}}^{-4}$ for every element along the diagonal,

$$\text{variance}(\mathbf{C}) \leq \frac{1}{(1 - (\alpha + 1)\epsilon)^2} \text{variance}(\mathbf{A}). \quad (60)$$

Next we analyze the bias. This part of the proof follows the structure of the proof of Theorem 1 in Alaoui and Mahoney (2015). It will be useful to analyze the quantity,

$$\begin{aligned} \|(1-\epsilon)\mathbf{K}(\mathbf{C})\mathbf{y}^*\|_2 &= \|((1-\epsilon)\mathbf{K}(\mathbf{C}) - \mathbf{K}(\mathbf{A}) + \mathbf{K}(\mathbf{A})) \mathbf{y}^* \|_2 \\ &\stackrel{(61)}{\leq} \|((1-\epsilon)\mathbf{K}(\mathbf{C}) - \mathbf{K}(\mathbf{A})) \mathbf{y}^* \|_2 + \|\mathbf{K}(\mathbf{A})\mathbf{y}^*\|_2, \end{aligned}$$

where the last line is due to the triangle inequality. Furthermore,

$$(1-\epsilon)\mathbf{K}(\mathbf{C}) - \mathbf{K}(\mathbf{A}) = \mathbf{K}(\mathbf{C}) \left((1-\epsilon)\mathbf{K}(\mathbf{A})^{-1} - \mathbf{K}(\mathbf{C})^{-1} \right) \mathbf{K}(\mathbf{A}), \quad (62)$$

so

$$\begin{aligned} &\| ((1-\epsilon)\mathbf{K}(\mathbf{C}) - \mathbf{K}(\mathbf{A})) \mathbf{y}^* \|_2 = \\ &= \| \mathbf{K}(\mathbf{C}) \left((1-\epsilon)\mathbf{K}(\mathbf{A})^{-1} - \mathbf{K}(\mathbf{C})^{-1} \right) \mathbf{K}(\mathbf{A})\mathbf{y}^* \|_2 \\ &\leq \| \mathbf{K}(\mathbf{C}) \left((1-\epsilon)\mathbf{K}(\mathbf{A})^{-1} - \mathbf{K}(\mathbf{C})^{-1} \right) \|_{\text{op}} \| \mathbf{K}(\mathbf{A})\mathbf{y}^* \|_2, \end{aligned} \quad (63)$$

where op refers to the operator norm $\|\mathbf{A}\|_{\text{op}} = \inf\{c \geq 0 : \|\mathbf{A}\mathbf{v}\| \leq c\|\mathbf{v}\| \forall \mathbf{v} \in V\}$, where V, W are a normed vector spaces and \mathbf{A} is a linear map from $\mathbf{A} : V \rightarrow W$. We also have,

$$\begin{aligned} &\| \mathbf{K}(\mathbf{C}) \left((1-\epsilon)\mathbf{K}(\mathbf{A})^{-1} - \mathbf{K}(\mathbf{C})^{-1} \right) \|_{\text{op}}^2 = \\ &= \| \mathbf{K}(\mathbf{C}) \left((1-\epsilon)\mathbf{K}(\mathbf{A})^{-1} - \mathbf{K}(\mathbf{C})^{-1} \right)^2 \mathbf{K}(\mathbf{C}) \|_{\text{op}}. \end{aligned} \quad (64)$$

From Eqn. 54, we have

$$(1-\epsilon)\mathbf{K}(\mathbf{A})^{-1} - \mathbf{K}(\mathbf{C})^{-1} \preceq \frac{\alpha\epsilon}{k} \|\mathbf{A}_{\setminus k}\|_F^2 \mathbf{I}, \quad (65)$$

which is squareable because $(1-\epsilon)\mathbf{K}(\mathbf{A})^{-1} - \mathbf{K}(\mathbf{C})^{-1}$ commutes with the identity. So,

$$\begin{aligned} &\| \mathbf{K}(\mathbf{C}) \left((1-\epsilon)\mathbf{K}(\mathbf{A})^{-1} - \mathbf{K}(\mathbf{C})^{-1} \right) \|_{\text{op}}^2 \\ &\leq \frac{\alpha^2\epsilon^2}{k^2} \|\mathbf{A}_{\setminus k}\|_F^4 \|\mathbf{K}(\mathbf{C})^2\|_{\text{op}} \\ &\leq \frac{\alpha^2\epsilon^2}{k^2} \|\mathbf{A}_{\setminus k}\|_F^4 \|\mathbf{K}(\mathbf{C})\|_{\text{op}}^2 \\ &\leq \frac{\alpha^2\epsilon^2 \|\mathbf{A}_{\setminus k}\|_F^4}{\|\mathbf{C}_{\setminus k}\|_F^4} \\ &\leq \frac{\alpha^2\epsilon^2}{(1-\alpha\epsilon)^2}. \end{aligned} \quad (66)$$

The second to last line follows from the definition of the operator norm and $\mathbf{K}(\mathbf{C})$. The last line follows from Eqn. 53.

Returning to Eqn. 61 gives,

$$\begin{aligned} \|\mathbf{K}(\mathbf{C})\mathbf{y}^*\|_2 &\leq \frac{1}{(1-\epsilon)} \left(\frac{\alpha\epsilon}{(1-\alpha\epsilon)} + 1 \right) \|\mathbf{K}(\mathbf{A})\mathbf{y}^*\|_2 \\ \|\mathbf{K}(\mathbf{C})\mathbf{y}^*\|_2 &\leq \frac{1}{(1-\epsilon)(1-\alpha\epsilon)} \|\mathbf{K}(\mathbf{A})\mathbf{y}^*\|_2. \end{aligned} \quad (67)$$

Therefore, using Eqn. 53 again,

$$\text{bias}(\mathbf{C}) \leq \frac{1}{(1-\epsilon)^2(1-\alpha\epsilon)^2} \text{bias}(\mathbf{A}). \quad (68)$$

Combining Eqn. 60 and Eqn. 68 gives,

$$\mathcal{R}(\hat{\mathbf{y}}_{\mathbf{C}}) \leq \max \left(\left(\frac{1}{1-(\alpha+1)\epsilon} \right)^2, \left(\frac{1}{1-\alpha\epsilon} \right)^2 \left(\frac{1}{1-\epsilon} \right)^2 \right) \mathcal{R}(\hat{\mathbf{y}}_{\mathbf{A}}). \quad (69)$$

On the interval $0 < \epsilon < \frac{1}{2\alpha}$, and for $\alpha > 1$,

$$\begin{aligned} &\max \left(\left(\frac{1}{1-(\alpha+1)\epsilon} \right)^2, \left(\frac{1}{1-\alpha\epsilon} \right)^2 \left(\frac{1}{1-\epsilon} \right)^2 \right) \\ &< 1 + \frac{2\alpha(-1+2\alpha+3\alpha^2)}{(1-\alpha)^2} \epsilon. \end{aligned} \quad (70)$$

Theorem 4 follows immediately.

5.8 Proof of Theorem 5

The proof is nearly identical to the proof of Theorem 3 of Papailiopoulos et al. (2014), so we do not repeat all of the algebra. It will be convenient to change notation. Without loss of generality, we can sort our column indices i in order of decreasing leverage score. We will also start this index at 1 instead of 0. With this change of notation, the power-law decay formula (Eqn. 15) becomes,

$$\bar{\tau}_i(\mathbf{A}) = (i)^{-a} \bar{\tau}_1(\mathbf{A}) \quad a > 1, \quad (71)$$

By the definition of the sum of ridge leverage scores and power-law decay (Eqn. 71),

$$\bar{t} = \bar{\tau}_1(\mathbf{A}) \sum_{i=1}^d i^{-a} \quad \rightarrow \quad \bar{\tau}_1 = \frac{\bar{t}}{\sum_{i=1}^d i^{-a}}. \quad (72)$$

By the definition of the DRLS algorithm, we collect $|\Theta|$ leverage scores such that $\bar{t} - \epsilon < \sum_{i \in \Theta} \bar{\tau}_i(\mathbf{A})$. This gives,

$$\bar{t} - \epsilon < \bar{\tau}_1 \sum_{i=1}^{|\Theta|} i^{-a} = \frac{\bar{t}}{\sum_{i=1}^d i^{-a}} \sum_{i=1}^{|\Theta|} i^{-a} \rightarrow \epsilon = \bar{t} \frac{\sum_{i=|\Theta|+1}^d i^{-a}}{\sum_{i=1}^d i^{-a}}. \quad (73)$$

Papailiopoulos et al. (2014) show that,

$$\frac{\sum_{i=|\Theta|+1}^d i^{-a}}{\sum_{i=1}^d i^{-a}} \leq \max \left(\frac{2}{(|\Theta|+1)^a}, \frac{2}{(a-1)(|\Theta|+1)^{a-1}} \right) \quad a > 1. \quad (74)$$

Noting that $\bar{t} \leq 2k$, substituting Eqn. 74 into Eqn. 73, solving for $|\Theta|$, and noting that the algorithm collects a minimum of k columns results in the expression for the number of columns collected when ridge leverage scores exhibit a power-law decay (Eqn. 15).

6 Conclusion

We extend deterministic feature selection from rank- k subspace leverage scores to ridge leverage scores. Ridge leverage scores provide a natural and stable alternative to rank- k subspace leverage scores for decreasing the importance of small principle components. Deterministic algorithms provide interpretability over their randomized counterparts.

We provide guarantees on the performance of our deterministic algorithm with respect to $(1 + \epsilon)$ error column subset selection, $(1 + \epsilon)$ error projection-cost preservation, and an additive-multiplicative spectral bound. These guarantees improve upon the available guarantees for deterministic feature selection with rank- k subspace leverage scores, and are comparable to randomized ridge leverage score algorithms under the assumption of power-law decay. We also show a $(1 + \epsilon)$ error guarantee on the statistical risk for ridge regression with a particular regularization constant and using the column subset from our deterministic algorithm. A similar ridge regression risk bound holds for randomized ridge leverage sampling. Lastly, we include a biological application to show that ridge leverage score power-law decay exists in the wild.

Acknowledgements

Research reported in this publication was supported by the National Human Genome Research Institute of the National Institutes of Health under Award Number F32HG008713. The content is solely the responsibility of the authors and does not necessarily represent the official views of the National Institutes of Health. SRM thanks Michael Mahoney, Ahmed El Alaoui, and Elaine Angelino for thoughtful comments and the Barcellos and Pachter Labs.

Supporting Information

Software in the form of python and R code is available at <https://github.com/srmcc/deterministic-ridge-leverage-sampling>. Code for downloading the data and reproducing all of the figures is included.

References

Ahmed El Alaoui and Michael W. Mahoney. 2015. Fast Randomized Kernel Ridge Regression with Statistical Guarantees. In *Proceedings of the 28th International Conference on Neural Information Processing Systems - Volume 1 (NIPS'15)*. MIT Press, Cambridge, MA, USA, 775–783. <http://dl.acm.org/citation.cfm?id=2969239.2969326> <http://arxiv.org/abs/1411.0306>.

Christos Boutsidis, Petros Drineas, and Malik Magdon-Ismail. 2011. Near-Optimal Column-Based Matrix Reconstruction. *arXiv:1103.0995 [cs]* (March 2011). <http://arxiv.org/abs/1103.0995> arXiv: 1103.0995.

Christos Boutsidis, Petros Drineas, and Michael W Mahoney. 2009. Unsupervised Feature Selection for the k-means Clustering Problem. In *Advances in Neural Information Processing Systems 22*, Y. Bengio, D. Schuurmans, J. D. Lafferty, C. K. I. Williams, and A. Culotta (Eds.). Curran Associates, Inc., 153–161. <http://papers.nips.cc/paper/3724-unsupervised-feature-selection-for-the-k-means-clustering-problem.pdf>

Leo Breiman. 1996. Heuristics of instability and stabilization in model selection. *The Annals of Statistics* 24, 6 (Dec. 1996), 2350–2383. <https://doi.org/10.1214/aos/1032181158>

Broad Institute of MIT and Harvard. 2016. Broad Institute TCGA Genome Data Analysis Center (2016): Analysis-ready standardized TCGA data from Broad GDAC Firehose 2016_01_28 run. (Jan. 2016). <https://doi.org/10.7908/C11G0KM9> Dataset.

Samprit Chatterjee and Ali S. Hadi. 1986. Influential Observations, High Leverage Points, and Outliers in Linear Regression. *Statist. Sci.* 1, 3 (Aug. 1986), 379–393. <https://doi.org/10.1214/ss/1177013622>

Michael B. Cohen, Sam Elder, Cameron Musco, Christopher Musco, and Madalina Persu. 2015. Dimensionality Reduction for k-Means Clustering and Low Rank Approximation. In *Proceedings of the Forty-seventh Annual ACM Symposium on Theory of Computing (STOC '15)*. ACM, New York, NY, USA, 163–172. <https://doi.org/10.1145/2746539.2746569>

Michael B. Cohen, Cameron Musco, and Christopher Musco. 2017. Input Sparsity Time Low-rank Approximation via Ridge Leverage Score Sampling. In *Proceedings of the Twenty-Eighth Annual ACM-SIAM Symposium on Discrete Algorithms (SODA '17)*. Society for Industrial and Applied Mathematics, Philadelphia, PA, USA, 1758–1777. <http://dl.acm.org/citation.cfm?id=3039686.3039801>

Petros Drineas, Michael W. Mahoney, and S. Muthukrishnan. 2008. Relative-Error CUR Matrix Decompositions. *SIAM J. Matrix Anal. Appl.* 30, 2 (Sept. 2008), 844–881. <https://doi.org/10.1137/07070471X>

C. Eckart and G. Young. 1936. The approximation of one matrix by another of lower rank. *Psychometrika* 1 (1936), 211–218. <https://doi.org/10.1007/BF02288367>

D. Feldman, M. Schmidt, and C. Sohler. 2013. Turning Big data into tiny data: Constant-size coresets for k-means, PCA and projective clustering. In *Proceedings of the Twenty-Fourth Annual ACM-SIAM Symposium on Discrete Algorithms*. Society for Industrial and Applied Mathematics, 1434–1453. <https://doi.org/10.1137/1.9781611973105.103>

Arthur E. Hoerl and Robert W. Kennard. 1970. Ridge Regression: Biased Estimation for Nonorthogonal Problems. *Technometrics* 12, 1 (Feb. 1970), 55–67. <https://doi.org/10.1080/00401706.1970.10488634>

Roger A. Horn and Charles R. Johnson. 2013. *Matrix analysis* (2nd ed ed.). Cambridge University Press, New York.

Shannon McCurdy, Vasilis Ntranos, and Lior Pachter. 2017. Column subset selection for single-cell RNA-Seq clustering. *bioRxiv* (July 2017), 159079. <https://doi.org/10.1101/159079>

Francesco Mezzadri. 2006. How to generate random matrices from the classical compact groups. *Notices of the American Mathematical Society* 54 (Oct. 2006).

Dimitris Papailiopoulos, Anastasios Kyrillidis, and Christos Boutsidis. 2014. Provable Deterministic Leverage Score Sampling. In *Proceedings of the 20th ACM SIGKDD International Conference on Knowledge Discovery and Data Mining (KDD '14)*. ACM, New York, NY, USA, 997–1006. <https://doi.org/10.1145/2623330.2623698>

The Cancer Genome Atlas Research Network. 2015. Comprehensive, Integrative Genomic Analysis of Diffuse Lower-Grade Gliomas. *The New England journal of medicine* 372, 26 (June 2015), 2481–2498. <https://doi.org/10.1056/NEJMoa1402121>

Robert Tibshirani. 1994. Regression Shrinkage and Selection Via the Lasso. *Journal of the Royal Statistical Society, Series B* 58 (1994), 267–288.

Paul F. Velleman and Roy E. Welsch. 1981. Efficient Computing of Regression Diagnostics. *The American Statistician* 35, 4 (1981), 234–242. <https://doi.org/10.2307/2683296>

Ying-Wooi Wan, Genevera I. Allen, and Zhandong Liu. 2016. TCGA2STAT: simple TCGA data access for integrated statistical analysis in R. *Bioinformatics* 32, 6 (March 2016), 952–954. <https://doi.org/10.1093/bioinformatics/btv677>

Jianhua Zhang. 2015. CNTTools: Convert segment data into a region by sample matrix to allow for other high level computational analyses. (2015). <http://bioconductor.org/packages/CNTTools/> R package version 1.26.0.

Hui Zou and Trevor Hastie. 2005. Regularization and variable selection via the Elastic Net. *Journal of the Royal Statistical Society, Series B* 67 (2005), 301–320.

Hui Zou and Hao Helen Zhang. 2009. On the adaptive elastic-net with a diverging number of parameters. *The Annals of Statistics* 37, 4 (Aug. 2009), 1733–1751. <https://doi.org/10.1214/08-AOS625>

Figures

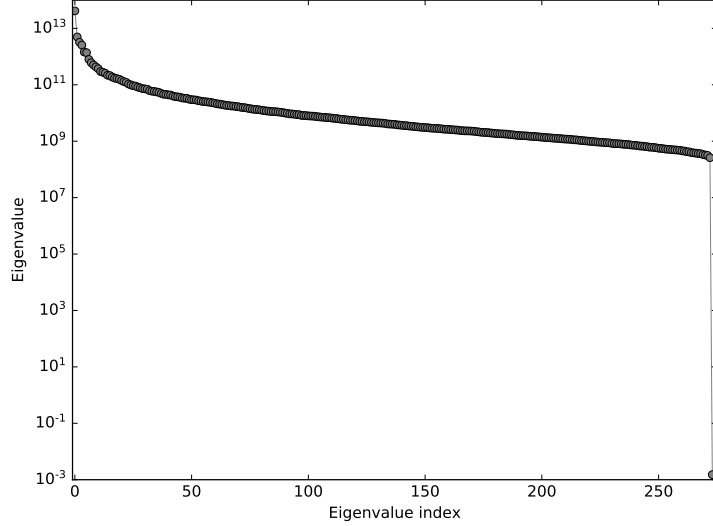


Figure 1: Eigenvalues of matrix $\mathbf{A}\mathbf{A}^T$ for LGG tumor multi-omic data. The eigenvalues range over multiple orders of magnitude.

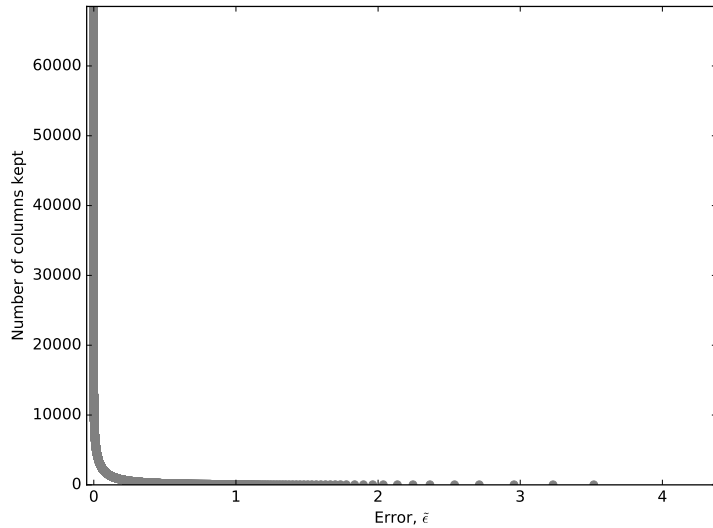


Figure 2: The error $\tilde{\epsilon}$ vs. the number of columns kept for LGG tumor multi-omic data $k = 3$ ridge leverage scores. A dramatic reduction in the number of columns kept incurs only a small error penalty.

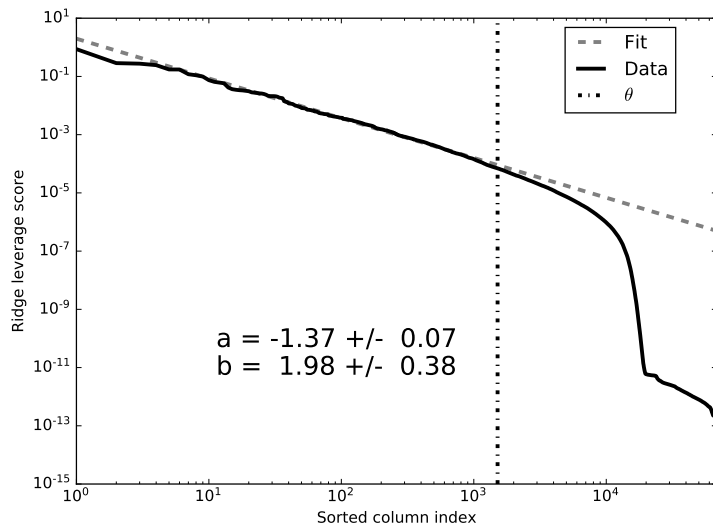


Figure 3: Power-law decay of LGG tumor multi-omic data $k = 3$ ridge leverage scores with sorted column index. The fit is to $\text{Score} = b \times (\text{Index})^a$ on the first 10^3 ridge leverage scores.

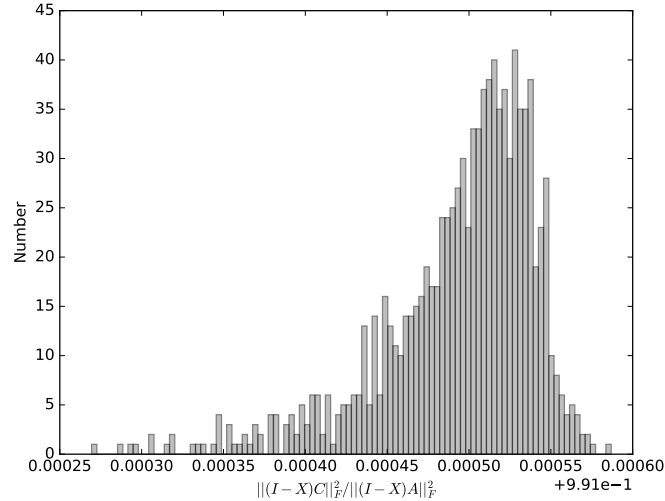


Figure 4: Histogram of $\|\mathbf{C} - \mathbf{X}\mathbf{C}\|_F^2 / \|\mathbf{A} - \mathbf{X}\mathbf{A}\|_F^2$ for 1000 random rank- $k = 3$ orthogonal projections \mathbf{X} and \mathbf{C} selected by the $k = 3, \epsilon = 0.1$ DRLS algorithm for LGG tumor multi-omic data.

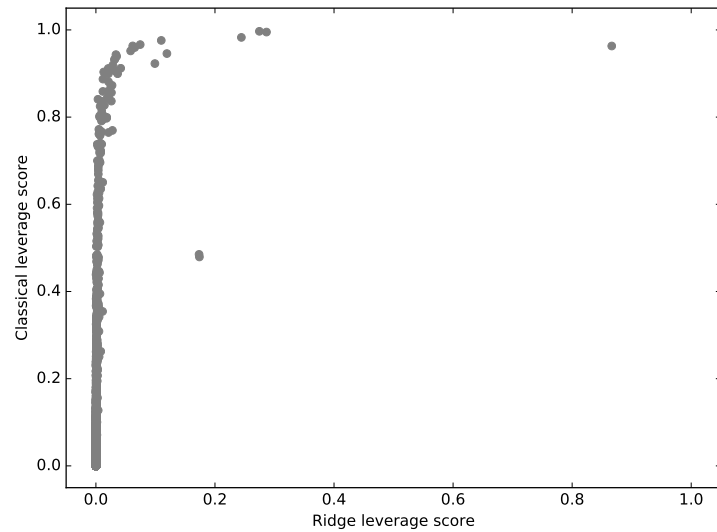


Figure 5: Classical leverage scores vs. $k = 3$ ridge leverage scores for LGG tumor multi-omic data. Most columns with large classical leverage scores have small ridge leverage scores; there is significant shrinkage.

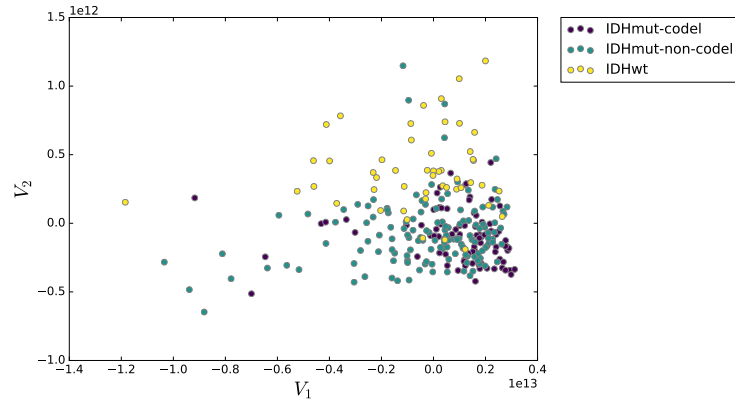


Figure 6: SVD projection of LGG tumor multi-omic data, colored by the combined status for "IDH" and "codel" outcome variables.

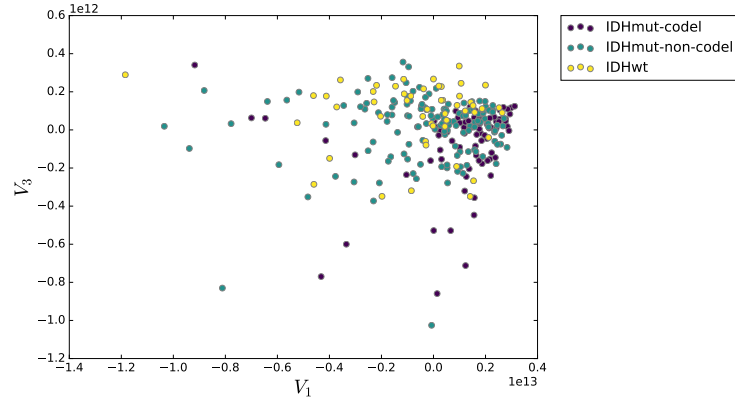


Figure 7: SVD projection of LGG tumor multi-omic data, colored by the combined status for "IDH" and "codel" outcome variables.

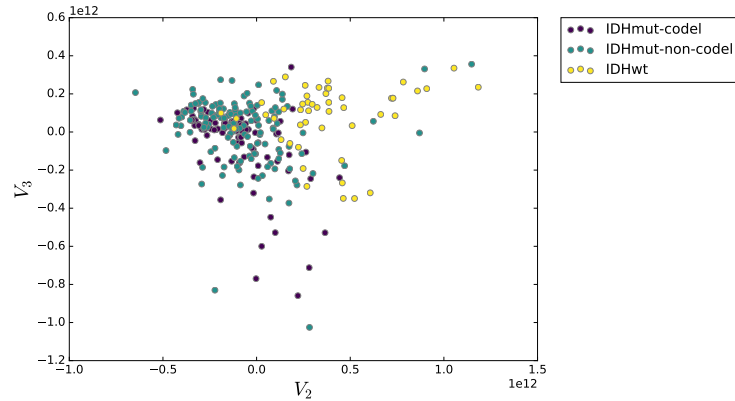


Figure 8: SVD projection of LGG tumor multi-omic data, colored by the combined status for "IDH" and "codel" outcome variables.

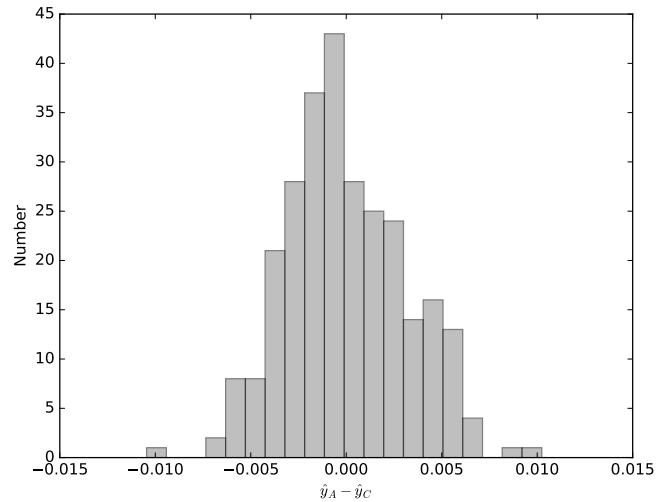


Figure 9: Histogram of $\hat{y}_A - \hat{y}_C$ for the outcome "codel."

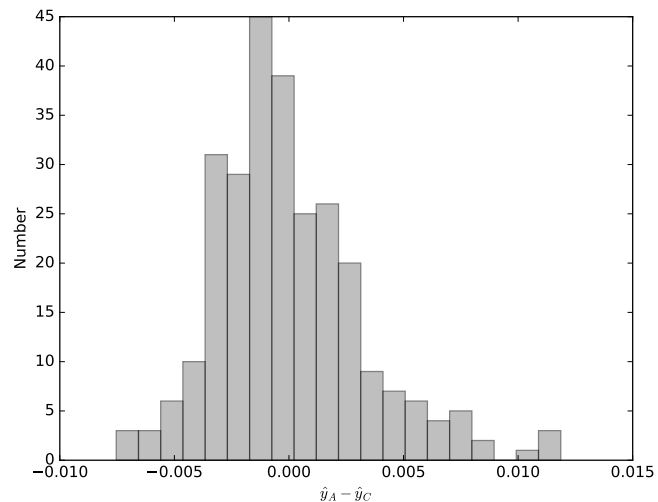


Figure 10: Histogram of $\hat{y}_A - \hat{y}_C$ for the outcome "IDH."

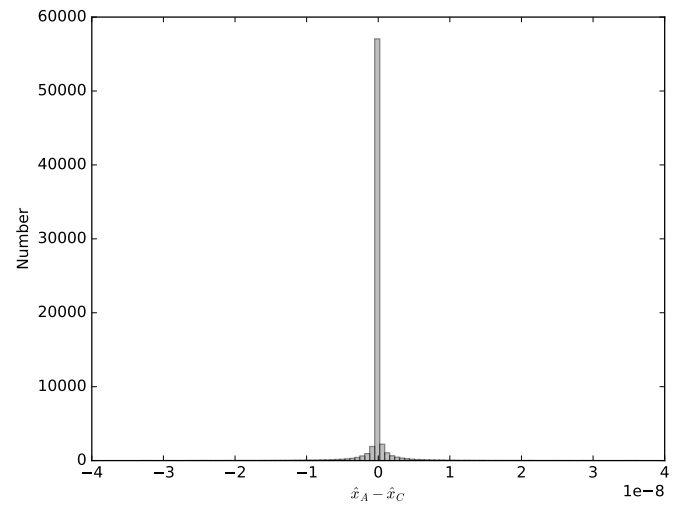


Figure 11: Histogram of $\hat{x}_A - \hat{x}_C$ for the outcome "code1."

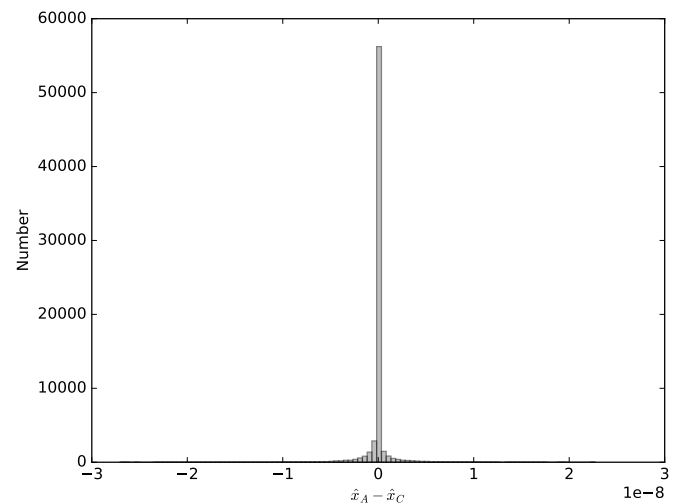


Figure 12: Histogram of $\hat{x}_A - \hat{x}_C$ for the outcome "IDH."

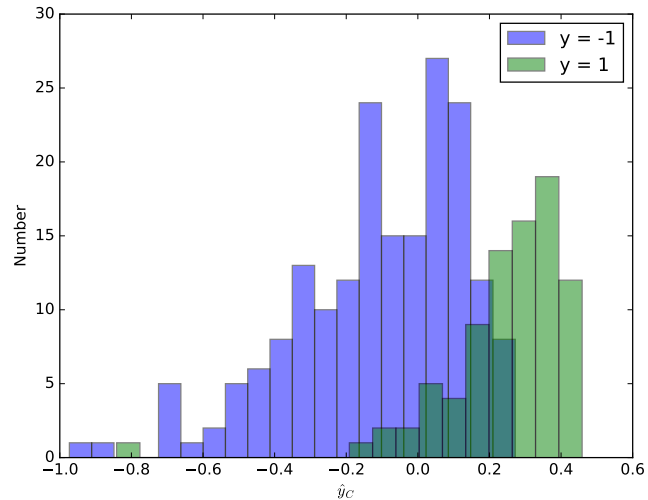


Figure 13: Histograms of the predictions \hat{y}_C conditioned the outcome y for "codel."

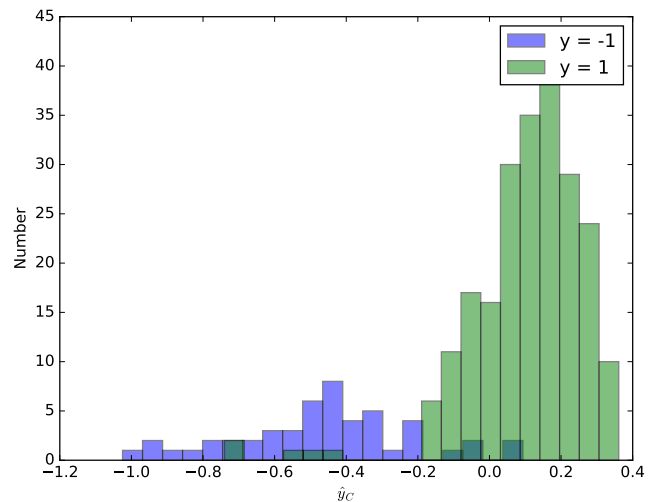


Figure 14: Histograms of the predictions \hat{y}_C conditioned on the outcome y for "IDH."